Effect of low initial pressures on ignition properties of lean n-decane/air mixtures for laser induced breakdown

Steve RUDZ[1], Pietro TADINI[1], Fanny BERTHET[1], Philippe GILLARD[1]
[1] Univ. Orléans, INSA-CVL, Laboratoire PRISME EA 4229
IUT de Bourges, 63 Avenue du Maréchal de Lattre de Tassigny, 18020 BOURGES, France.

1 Introduction

During the last twenty years, the interest on laser ignition for applications in aerospace propulsion has significantly grown, due to the several advantages demonstrated with respect to conventional electrical spark igniters [1]. In fact, besides the possibility to precisely control the input energy, a laser-induced spark ignition provides a more stable combustion, characterized by lower fuel consumption and decrease of pollution products emission [2]. Furthermore, lean fuel mixtures can be easily ignited, as well as ignition of high and low pressure mixtures, and multi-point laser sparks reduce the ignition delay time [1,2,3]. In practice, this features promise the achieving of higher performance for the commonly employed aviation engines, spanning from internal combustion to turbofan motors. In particular, the former takes a great advantage from laser ignition, since it does not disturb the cylinder geometry and, more important, eliminates the quenching on flame kernel provoked by electrodes [1]. Another result of interest in using laser instead of spark plug is that it can extend the lean flammability limit defined with spark plug [4]. The elimination of kernel cooling with electrode-less ignition represents a key feature for the development of hypersonic flight systems (i.e. scramjet), whose combustion occurs in a supersonic flow, hence the characteristic times of chemical reactions are required be smaller than that of fluid dynamics. In this context, the possibility to improve the combustion stability at high Mach should lead overcome the actual limits of the flight envelope, toward region of lower dynamic pressure (0.05-0.2 atm) [1,5]. Therefore, laser ignition is a key technology for improvement and development of actual and future aviation systems, also characterized by further, more practical, benefits, such as a simple maintenance and lower reparation costs [1].

This work deals with the ignition energy characterization, by laser-induced spark, of mixtures made by air and n-decane-99%. In fact, the latter is the main constituent of kerosene, thus used as its surrogate for combustion analysis. Nowadays, in civil aviation, customers ask for more stringent requirements on new turbofan engines; for instance, pollution emission reduction and less fuel consumption. Particular interest is toward engine relight capability by only exploiting windmilling, after a total power loss in flight and prolonged inactivity, with consequently combustor and fuel temperature decrease [6,7,8]. Indeed, after a flameout, a certain turbo-machinery rotation can be sustained by the static pressure in front of the fan and, despite the significant pressure loss in the combustion chamber, in certain conditions the engine relighting

Correspondence to: steve.rudz@univ-orleans.fr

is achievable without the need of the Auxiliary Power Unit (APU) [8]. To this end, the velocity of the inlet flow must be enough to provide a sufficient fuel atomization, which, due to temperature lowering, results more viscous and less volatile. On the contrary, too higher flow velocity hampers the stabilization of the flame (blow out) in the primary combustion zone. Engine relighting capability are limited within a windmill flight envelope, which defines the upper possible altitude depending on sub-atmospheric pressure range, typically between 0.94 and 0.35 atm [7], and oxidizer density required [8].
The abovementioned benefits of laser-induced spark ignition might represent a valuable solution for this kind of application; the ignition of lean fuel mixtures at sub-atmospheric pressure might theoretically allow an improvement of the windmill envelope boundaries with respect to actual engines equipped with conventional igniters.

2 Experimental apparatus

In Figure 1, a schematic view of the experimental setup is presented. A detailed description of the vessel, energy meter, laser, as well as their combination, is available in [9], thus providing here, just a synthetic remind. The Gaussian laser beam, generated by a Quantel Brilliant Nd:Yag (λ = 1064 nm, D = 6 mm, M^2 = 1.75, pulse duration τ_{FWHM} = 4.48 ns), is sent to the closed cylindrical vessel (length = 200 mm, internal diameter = 80 mm). Prior entering in the test chamber, the beam is firstly expanded 3 times by lens 1 and 2 (see Figure 1), secondly a small amount is split toward the first energy meter, used to measure the input energy, whereas the rest of the beam is focused into the center of the vessel with a coated plano-convex lens, characterized by focal length of f_3 = 150 mm. At the opposite output of the vessel a second energy meter measures the transmitted energy. With regard to the gaseous mixture, n-decane, provided by Alfa-Aesar (A14732 n-Decane, 99%), is used as fuel, while synthetic air made by 20% O_2 and 80% N_2 (Air Liquid ALPHAGAZ 1), as oxidizer.

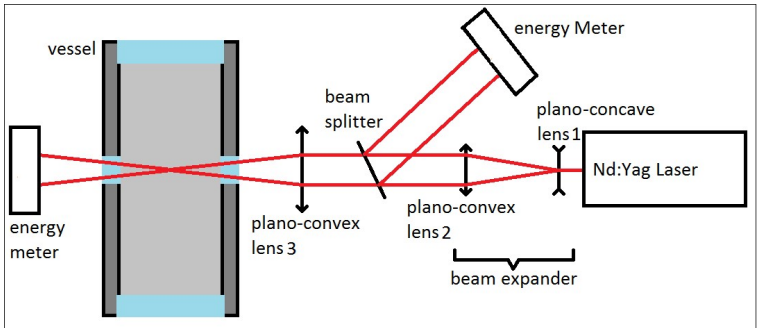

Figure 1. Schematic view of the experimental set-up.

3 Experimental protocol

In this work, five equivalence ratios Φ = {0.65, 0.8, 0.9, 1.1, 1.3} at different static pressure P = {0.2, 0.3, 0.4, 0.5, 0.8, 1, 1.5, 2} atm and with temperature of 347 K are investigated. To analyze each configuration, the Langlie method [10], with a log-normal law, is considered, since this statistical approach generally needs only 20-25 shots to provide a valid empirical relation between ignition probability incident energy [11]. Basically, this method looks for the raw E_{50} (energy needed to obtain 50% probability of ignition) by a dichotomy approach, also allowing the calculation of the corresponding raw standard deviation σ_0:

$$\text{raw } E_{50} = \frac{X_m + X_M}{2} \text{ and } \sigma_0 = N\frac{\ln(X_m) - \ln(X_M)}{8(n+2)} \quad (1)$$

where X_m is the lowest energy leading to ignition, X_M the highest energy leading to no-ignition, N the total number of shots and n the number of shots occurred between $[X_m ; X_M]$.
Then, a fitting of experimental results to the cumulative distribution function of a log-normal law, whose equation is:

$$F_{\log}(E) = \frac{1}{2}\left(1 + \mathrm{erf}\left(\frac{\ln(E) - \mu}{\sqrt{2}\sigma}\right)\right) \quad (2)$$

where μ and σ are respectively the mean and the standard deviation of the variable's natural logarithm (i.e. the energy).
Finally, one can deduce the corrected values of E_{50}:

$$E_{50} = \exp(\mu) \quad (3)$$

4 Results and discussions

In the laser-spark ignition experiments, as carried out in this work, the Langlie method needed between 20 to 30 shots for converging to the E_{50} value of incident energy. The estimated E_{50} is reported in Table 1, as a function of the initial chamber pressure P and the mixture equivalence ratio Φ.

Table 1: E_{50} [mJ] referred to the different investigated conditions (Φ ; P).

Φ \ P	**0.2**	**0.3**	**0.4**	**0.5**	**0.8**	**1**	**1.5**	**2**	**2.5**
0.65	*no ignition*	141.65	77.51	***36.41***	39.64	43.96	57.22	80.87	153.98
0.8	138.3	58.89	*no test*	29.56	21.03	***13.66***	17.23	18.82	24.48*
0.9	87.39	41.41	*no test*	23.02	17.16	12	9.39	***9.07***	13.00*
1.1	57.49	30.31	*no test*	17.18	11.43	7.93	***7.1***	***7.04****	*no test*
1.3	50.83	27.3	*no test*	14.99	8.63	***7.32***	***6.35****	*no test*	*no test*

The results denoted with * indicates that not all the injected n-decane was vaporized in the tested condition due to a higher expected partial pressure than the saturation one. In Figure 2, one can see the variation of E_{50} with pressure, for different equivalence ratios, whereas in Figure 3, the E_{50} change is presented as a function of the equivalence ratio, for the considered pressure values. Thus, focusing only on fully vaporized cases, the E_{50} decreases when P increases for the richest mixture (Φ = 1.1 and 1.3), while the leanest equivalent ratio is more likely described by a U-shape trend (see Figure 2). With regard to equivalence ratios 0.8 and 0.9, E_{50} drastically decreases between 0.2 and 1 atm, remains then almost constant, despite a slight increase when P increases after 1 atm. Concerning the not fully vaporized tests, it is noticeable that it does not influence the trend revealed by the gaseous phase. It also appears that, for any given pressure, E_{50} decreases strongly when the equivalent ratio changes from 0.65 to 1.3 (see Figure 3).

During these experiments we observed that the used optical configuration leads to a smaller deviation of the absorbed energy by the plasma when a breakdown occurred. To investigate the correlation between the energy sent by the laser E_{inc} and the energy absorbed by the plasma E_{abs}, a power law is used:

$$E_{abs} = \alpha(E_{inc} - \delta)^{\beta} \quad (4)$$

where δ has the dimension of an energy and this mathematical offset, on the E_{inc} axis, could physically be considered as a minimum threshold value for achieving a breakdown.

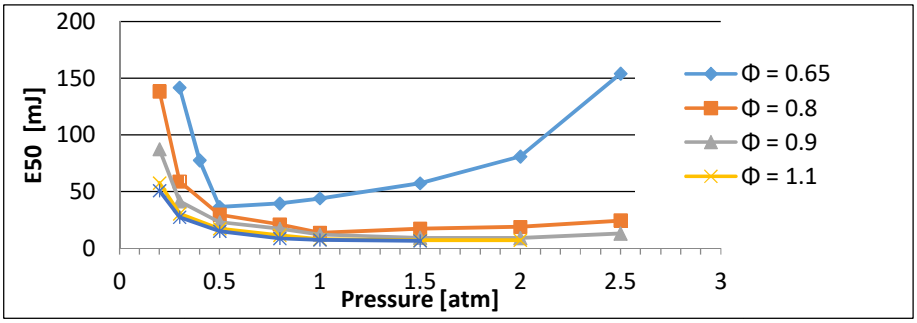

Figure 2. E_{50} vs initial vessel pressure P for different equivalence ratios.

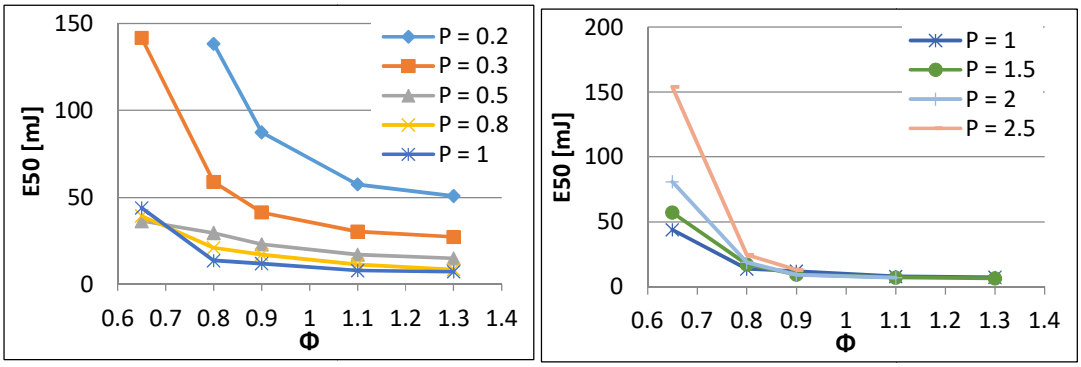

Figure 3. E_{50} vs equivalence ratio Φ for different initial vessel pressures. .

In all cases, the proposed fitting results in good agreement with experimental data; the values of the parameters α, β and δ are reported in Tables 2, 3 and 4 respectively. In Figure 4 two examples of this analysis are presented, where, for convenience, the ratio E_{abs}/E_{inc} is in function of E_{inc}. The deviation to the fitting curves, as observed in Figure 4, associated with the higher data dispersion, seems to increase at the lowest initial vessel pressures.

Concerning the coefficient α (see Table 2), the pressure effect is pronounced at low pressures whereas for values greater than 0.5 atm it is unclear to determine if variations are mainly due to pressure or to the equivalent ratio. The coefficient β (see Table 3) strongly depends on pressure from 0.2 to 1 atm. After this range β is constant to 1 for all tested pressures and equivalence ratios. On the other hand, the parameter δ is mainly influenced by pressure, as one can see in Table 4.

Table 2: parameter α for different test conditions (Φ ; P).

Φ \ P	**0.2**	**0.3**	**0.4**	**0.5**	**0.8**	**1**	**1.5**	**2**	**2.5**
0.65	*no ignition*	0.74	1.04	0.98	1.00	1.00	0.95	0.96	0.95
0.8	0.47	0.69	*no test*	1.02	0.87	0.84	0.86	0.95	0.99*
0.9	0.52	0.67	*no test*	0.83	0.79	1.07	0.93	0.96	0.91*
1.1	0.42	0.71	*no test*	0.95	1.13	1.04	0.92	0.88*	*no test*
1.3	0.46	0.90	*no test*	0.90	0.87	0.92	0.92*	*no test*	*no test*

Table 3: parameter β for different test conditions (Φ ; P).

Φ \ P	**0.2**	**0.3**	**0.4**	**0.5**	**0.8**	**1**	**1.5**	**2**	**2.5**
0.65	*no ignition*	1.03	0.99	0.99	0.99	0.99	1.00	1.00	1.00
0.8	1.10	1.05	*no test*	0.99	1.02	1.02	1.01	1.00	0.99
0.9	1.10	1.05	*no test*	1.03	1.03	0.98	1.00	1.00	1.00
1.1	1.13	1.04	*no test*	1.00	0.97	0.98	1.00	1.01	*no test*
1.3	1.09	1.00	*no test*	1.01	1.02	1.00	1.00	*no test*	*no test*

Table 4: threshold parameter δ[mJ] for for different test conditions (Φ ; P).

Φ \ P	**0.2**	**0.3**	**0.4**	**0.5**	**0.8**	**1**	**1.5**	**2**	**2.5**
0.65	*no ignition*	11.11	12.61	9.70	8.00	6.81	5.89	5.18	4.15
0.8	12.55	11.70	*no test*	11.07	6.90	7.07	4.89	4.62	4.28*
0.9	15.93	11.70	*no test*	9.49	7.16	7.55	5.75	5.11	4.14*
1.1	10.78	11.3	*no test*	10.27	6.50	6.60	5.56	4.84*	*no test*
1.3	11.59	13.76	*no test*	9.71	6.53	6.13	5.24*	*no test*	*no test*

In order to validate this approach, the obtained mathematical offsets δ are investigated with by means of

$$\delta = A \times P^{a} \times \left[C_{10}H_{22}\right]^{b} \times \left[O_2\right]^{c} \times \left[N_2\right]^{d} \tag{5}$$

where A is a dimensionless coefficient, P is the pressure in atm and the molar concentrations [.] in mol.cm^{-3}. By exploiting a numerical optimization the parameters of Eq. 5 are calculated {A, a, b, c, d}={1.7744, -0.5037, -0.1444, -0.0542, 0.2631}. In the presented application $\delta \propto P^{-0.5}$ and according to [12] it is consistent to consider δ as an energy threshold.

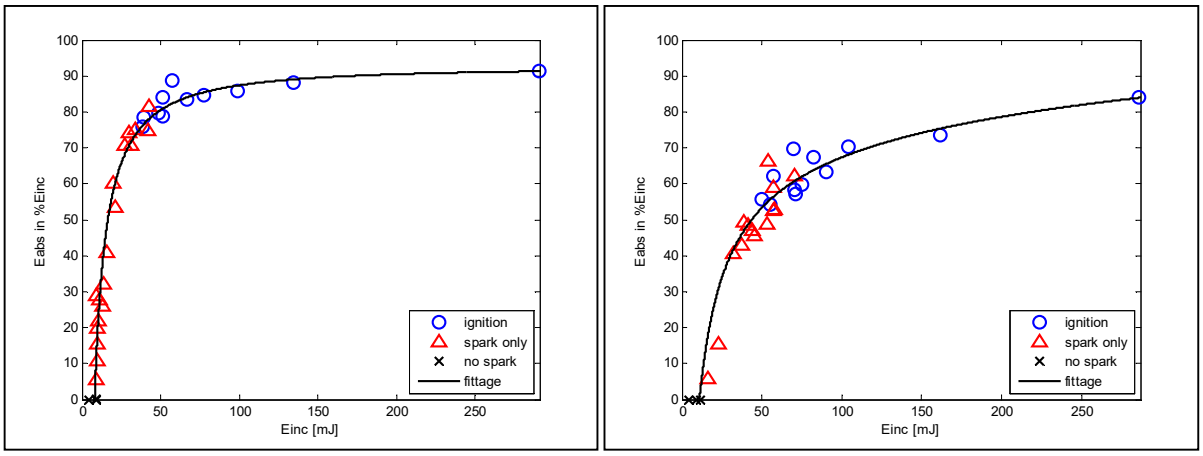

(a) (b)

Figure 4. E_{abs}/E_{inc} vs E_{abs}: (a) P = 0.8 bar and Φ = 0.65; (b) P = 0.2 bar and Φ = 1.1.

5 Conclusion and perspectives

The presented experimental results analyze the ignition properties of n-decane/air mixtures for Φ from 0.65 to 1.3 and static initial chamber pressure ranging from 0.2 to 2.5 atm. On the one hand, presented results show that for a given initial pressure the energy required to reach E_{50} diminishes a lot when Φ increases from 0.65 to 1.3. On the other hand, the initial pressure effect on the E_{50} for a given equivalent ratio is not the same for all tested ones. A power law has been successfully used to predict the amount of absorbed energy by the n-decane/air mixture for a given incident energy, sent by the laser source, as well as an energy threshold value for each ignited test configuration. Next efforts will focus on kernel visualization of the flame development, by using the Schlieren method, to better understand the effect of the initial pressure.

Authors are grateful to Labex CAPRYSSES and CNRS FR 776 EPEE for their financial supports.

References

[1] O'Briant SA, Gupta SB, Vasu SS. (2016). Review: laser ignition for aerospace propulsion. Propulsion and Power Research 5 (1): 1.

[2] Weinrotter M, Kopecek H, Tesch M, Wintner E, Lackner M, Winter F. (2005). Laser ignition of ultra-lean methane/hydrogen/air mixtures at high temperature and pressure. Experimental Thermal and Fluid Science 29: 569.

[3] Pal A, Agarwal AK. (2015). Comparative study of laser ignition and conventional electrical spark ignition systems in a hydrogen fuelled engine. International Journal of Hydrogen Energy 40 (5): 2386.

[4] Xu C, Fang D, Luo Q, Ma J, Xie Y. (2014). A comparative study of laser ignition and spark ignition with gasoline–air mixtures. Optics & Laser Technology 64: 343.

[5] Starikovskaia SM. (2006). Plasma assisted ignition and combustion. Journal of Physics D: Applied Physics, 39 (16):0–12.

[6] EASA (2015) Certification Memorandum: turbine engine relighting in flight. Report EASA CM No.: CM-PIFS-010 Issue 01.

[7] von der Bank R, Donnerhack S, Rae A, Poutriquet F, Lundbladh A, Schweinberger A. (2015). Advanced core engine technologies assessment & validation. Proceedings of 11th European Conference on Turbomachinery Fluid dynamics & Thermodynamics ETC11, Madrid, Spain March 23-27.

[8] Weckering J. (2011). Development of numerical modeling methods for prediction of ignition processes in aero-engines. PhD Thesis, Technische Universität Darmstadt.

[9] Rudz S, Chetehouna K., Strozzi C, Gillard P. (2014). Minimum Ignition Energy Measurements for α-Pinene/Air Mixtures. Combustion Science and Technology, 186(10-11): 1597.

[10] Langlie HJ. (1962). A reliability test method for one shot items. Publication n_U. 1792. Ford Motor Company Aeronutronic.

[11] Bernard S, Lebecki K, Gillard P, Youinou L, Baudry G. (2010). Statistical method for the determination of the ignition energy of dust cloud-experimental validation. Journal of Loss Prevention in the Process Industries 23: 404.

[12] Phuoc TX, White FP. (1999). Laser-Induced Spark Ignition of CH4/Air Mixtures. Combustion and Flame 119: 203.